Asociación Argentina
de Mecánica Computacional

Mecánica Computacional Vol XXIX, págs. 10183-10195 (artículo completo)
Eduardo Dvorkin, Marcela Goldschmit, Mario Storti (Eds.)
Buenos Aires, Argentina, 15-18 Noviembre 2010

EFFECT OF STRESS-STRAIN RELATIONS ON THE NONLINEAR BEHAVIOR OF QUASI-BRITTLE STRUCTURES

Fabricio Zuleta[a], Raul R. Silva[b] and Glauco J. O. Rodrigues[c]

[a] *D.Sc. Student, Department of Civil Engineering Pontifícia Universidade Católica do Rio de Janeiro.*

[b] *Associate Professor, Chairman, Department of Civil Engineering, Pontifícia Universidade Católica do Rio de Janeiro.*

[c] *D.Sc., Adj. Prof. PUC-Rio, Eng. Furnas Centrais Eletricas.*

Keywords: Fracture energy, size effect, quasi-brittle materials.

Abstract. The fracture of quasi-brittle structures is modeled with two-dimensional finite elements with inclusion of special elements along a predefined crack. These special elements are rod elements with a nonlinear stress-strain diagram which allow for softening behavior, providing for gradual reduction of stress in the crack opening process. The fracture energy per unit of area, specified for the material, corresponds to the work performed in the rod elements. A general purpose finite element code with nonlinear analysis capability is used.
Results for standard three-point beam tests are obtained with use of nonlinear analysis with generalized displacement control, aiming to reproduce test results with use of a clip gage or similar device for the measuring of the crack mouth opening displacement (CMOD). Four beams of different sizes, with the same height/length ratio are analyzed with various levels of mesh refinement. An edge notch at mid span warrants the formation of a single crack normal to the beam axis.
Linear and bilinear softening diagrams are considered, with different fracture energies, applicable to concrete. The examples demonstrate the influence of the fracture energy and the shape of the stress-strain diagram on the representative features of structure behavior, such as maximum load, load-displacement curve and size effect.

1 INTRODUCTION

Several methods for modeling the process of fracture in quasi-brittle materials have been proposed. The cohesive crack model is practical and simple. In this method, the fracture process zone is modeled by a profile of stresses in front of the crack tip that gradually tends to zero as the crack advances. The behavior in the line of fracture can be modeled by one-dimensional elements (special frame elements) with softening stress-strain diagrams, and so take advantage of existing efficient commercial software.

The frame element available in the SAP2000 software was used for this purpose. The rest of the structure was modeled accordingly with shell elements that can also represent either stress or strain plane states.

Studies were performed in numerical tests of three point loaded beams. Four geometrically similar specimens with different sizes were used for comparison. The maximum load, the snap back in the load-deflection response and the fracture size effect were studied by varying the softening stress-strain diagram while keeping characteristic values of concrete properties.

2 COHESIVE CRACK METHOD

In the cohesive crack method the fracture process zone can be represented with interface elements that transmit stresses between the two faces where they are connected, Figure 1. These stresses follow a certain law that depends on the size of the opening crack displacement.

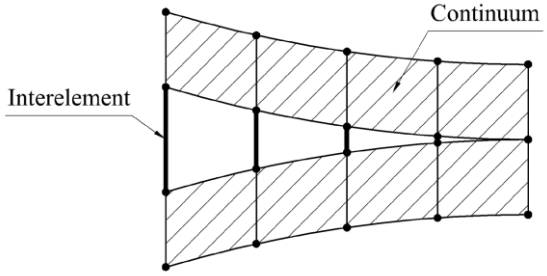

Figure 1: Discrete inter-element crack approach in the fracture process zone.

In this study frame elements can be used as interface elements, provided such elements have nonlinear properties corresponding to softening diagrams for monotonically increasing strain or other displacement-related quantity, Figure 2(a). In this way a typical stress-opening displacement can be reproduced as shown in Figure 2(b).

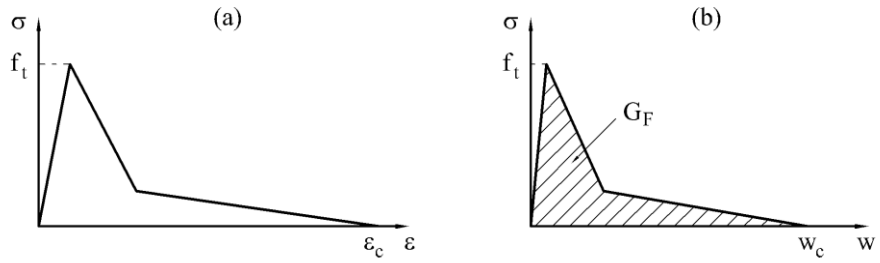

Figure 2: (a) Stress-strain diagram with bilinear softening, (b) Stress-opening displacement diagram.

In Figure 2, G_F stands for cohesive fracture energy, f_t is the tensile strength, w is the opening displacement of the crack, ε_c and w_c are the critical strain and the critical opening displacement, respectively, where the stress values reach zero.

The next equation relates the fracture energy with the softening diagrams.

$$G_F = L\int_0^{\varepsilon_u} \sigma \, d\varepsilon = \int_0^{w_u} \sigma \, dw \tag{1}$$

where L is the length of the element.

3 THREE POINT BEND BEAM AND SOFTENING CURVES

3.1 Three point bend beam

A three point bend beam test was analyzed that is widely used for determination of fracture energy in experimental tests, Figure 3. The cohesive fracture energy is calculated as the relation between the external work measured in the load-deflection diagram and the uncracked area (*5/6 d t*).

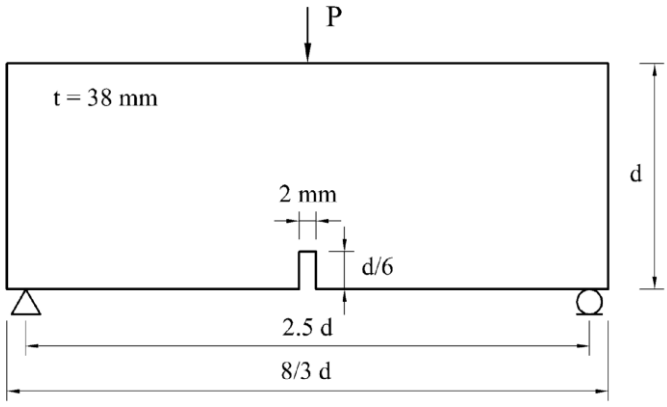

Figure 3: Dimensions used for a three point bend beam.

Four specimens geometrically similar were tested numerically with different fracture energies, varying the depth from 38, 76, 152 and 304 mm. Other depths were also included for determination of the size effect.

3.2 Softening curves

Several softening (post-peak) diagrams exist in the literature, the most common being the linear, bilinear and exponential or pseudo-exponential diagrams. In this work linear softening, Figure 4(a), was used for validation of the model and to show how the fracture energy influences the behavior of the load-deflection diagrams for different sizes. The bilinear diagram also was studied because it appears to be more suitable for modeling fracture in concrete, since it has been shown that the peak load of the overall structure is highly dependent of the initial post-peak slope. Thus, both the peak load and the fracture energy can be varied with the same maximum strain, Figure 4(b). The influence of the value σ_k (ordinate of the kink point) in the post-peak behavior will be further studied.

In the bilinear diagram the initial downward slope is related to the initial fracture energy G_f as shown in Figure 5, (Roesler et.al. 2007) .The recommended values for the relation σ_k / f_t are between 0.15 and 0.33 and G_F / G_f = 2.5 (Bažant 2002).

The values of ε_c and ε_k are determined by the eq. (2) and eq. (3) respectively.

$$\varepsilon_c = \frac{2}{L\,\sigma_k}\left[G_F - \left(1-\frac{\sigma_k}{f_t}\right)G_f\right] \tag{2}$$

$$\varepsilon_k = \frac{\sigma_k}{E} + \frac{2\,G_f}{L\,f_t}\left(1-\frac{\sigma_k}{f_t}\right) \tag{3}$$

with E = Young's modulus and the other values defined above.

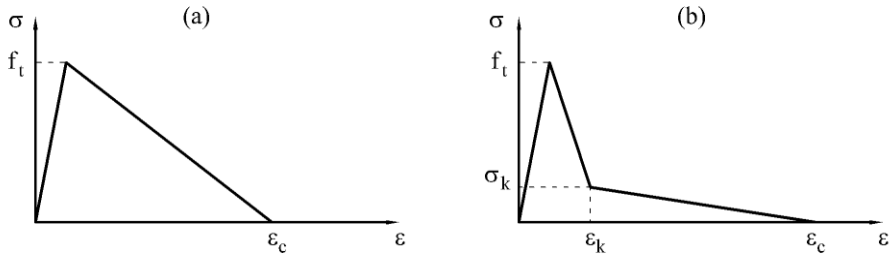

Figure 4: Stress-strain softening diagrams (a) linear, (b) bilinear.

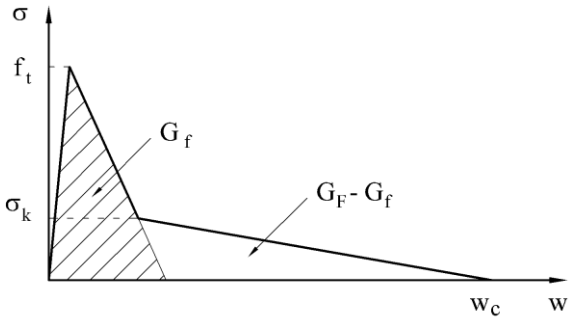

Figure 5: Bilinear stress-opening displacement diagram.

4 NUMERICAL ANALYSIS

4.1 Discretization

The beams have been modeled herein with shell elements, although elements type plane stress and plane strain, also provided by Sap2000, could be used since this is a two-dimensional analysis. Hence, rotational degrees of freedom are available in the model. The pre-defined line of fracture is modeled with frame elements with nonlinear behavior, as mentioned above, which act mostly as one-dimensional links.

An example of discretization for an 152 [mm] depth beam and the transversal cross section of a frame element are shown in the Figure 6, frame height H depends of the refinement of the mesh.

4.2 Nonlinear analysis

Once the stress-strain diagram is determined according to the parameters of the cohesive crack method, namely fracture energy G_F, tensile strength f_t and initial fracture energy G_f, this stress-strain diagram is assigned to frame elements that join the nodes along the pre-defined line of fracture.

A nonlinear analysis with adequate control must be employed. The displacement control adopted is a generalized displacement called Crack Mouth Opening Displacement (CMOD), Figure 7, where u_r and u_l are the horizontal displacements of the joints r and l respectively. This indirect displacement control is also used in experimental tests to obtain stable results.

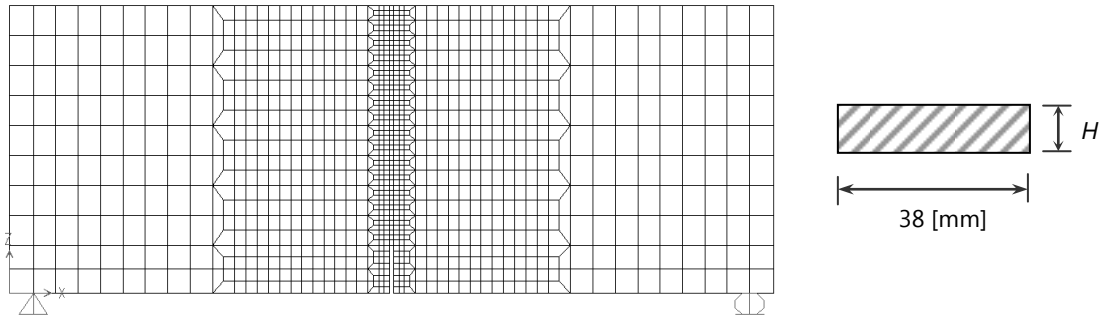

Figure 6: Beam's discretization and transversal cross section of a frame.

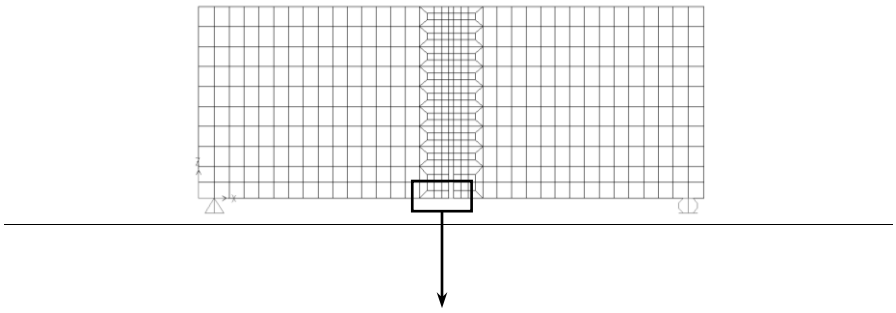

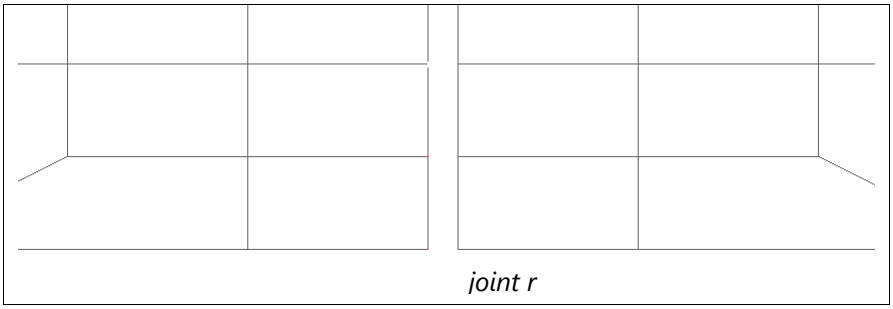

$$\delta_G = u_r - u_l$$

Figure 7: Generalized displacement.

An incremental-iterative method is performed by the program Sap2000 that allows for unloading the entire structure when a loss of stiffness is found. Internally the program prevents for sudden softening in the force-displacement diagrams (CSI Analysis reference manual, 2009), which can be a disadvantage when the fracture energy is smaller and therefore the slope down of the stress-strain diagram more inclined; in such cases the length of the frame can be reduced to overcome this constraint.

4.3 Material properties

Material properties compatible with concrete have been used: characteristic compression strength f_c = 88.34 [MPa], characteristic tension strength f_t = 5.64 [MPa], Young's modulus E = 38104 [MPa] and Poisson's coefficient ν = 0.20.

5 RESULTS FOR LINEAR SOFTENING DIAGRAMS

5.1 Response load-displacement curves

Four notched geometrically similar specimens in a three point bend test have been modeled with depths of 38, 76, 152 and 304 [mm]. The value of the fracture energy G_F = 150 [N/m] was used for construction of softening stress-strain diagrams for the frame elements.

The results are shown in Figure 8 and Figure 9; in the former the load is plotted vs. the generalized displacement (CMOD) and in the latter the load is plotted against the vertical load point displacement. The total external work can be graphically determined from Figure 9 for each beam, which allows the fracture energy to be recovered for validation of the numerical analysis. The results are summarized in Table 1.

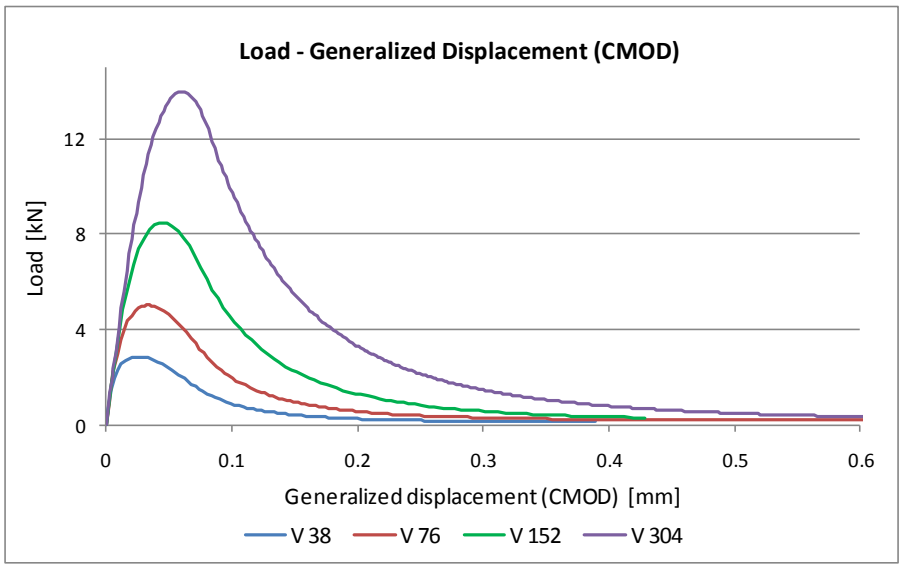

Figure 8: Load vs. generalized displacement for notched beams of 38, 76, 152 and 304 [mm] of depth.

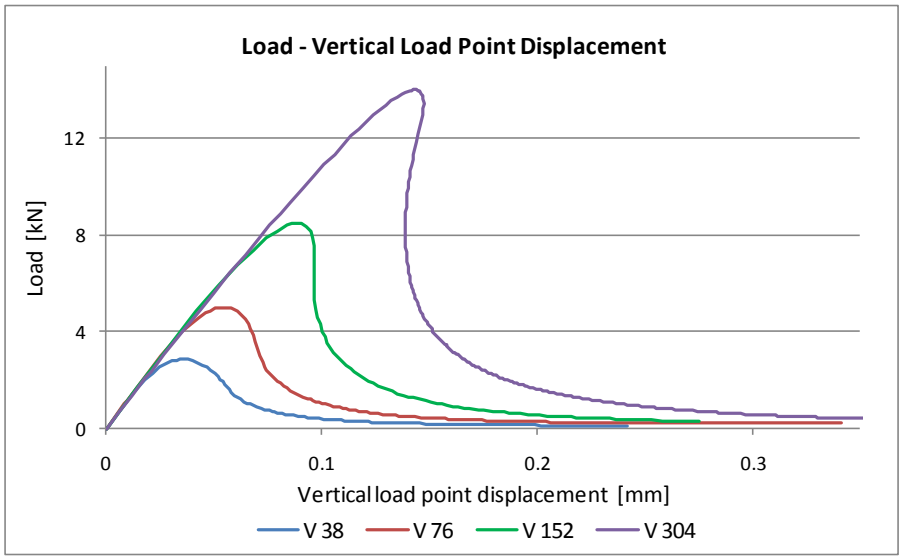

Figure 9: Load vs. vertical load point displacement for notched beams of 38, 76, 152 and 304 [mm] of depth.

Beams' depth [mm]	38	76	152	304
Peak load [kN]	2.86	5.01	8.49	14.16
Area below load-vertical displacement curve [N-m]	0.1766	0.3671	0.6782	1.4342
Fracture energy [N/m]	146.76	152.53	140.90	148.98

Table 1: Three point notched beam with linear softening diagram.

In the beam of 304 [mm] of depth, the fracture energy G_F was assumed to be

values of 100, 150 and 200 [N/m], the curves for load-vertical displacement are shown in the Figure 10 and the peak loads in the Table 2.

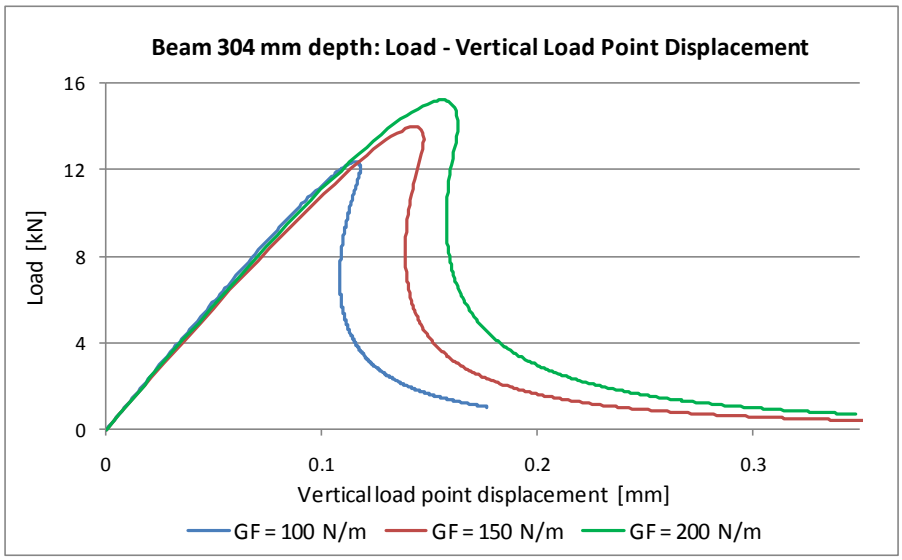

Figure 10: Load vs. vertical displacement for beams of 304 [mm] of depth with different fracture energies.

Fracture energy [N/m]	Peak load [kN]
100	12.36
150	14.16
200	15.22

Table 2: Peak loads in beams 38 [mm] depth with different fracture energies.

It can be observed that the peak load decreases when the fracture energy is reduced because the slope of the softening diagram becomes more inclined. This behavior is expected since there is experimental evidence of dependence of the peak load on the initial slope of the softening diagram, mainly in smaller specimens, (Bažant and Planas, 1998).

The beam with 38 [mm] of depth was modeled with different levels of mesh refinement, Figure 11. The resulting load-displacement curves are shown in Figure 12 and the values of peak load in Table 3.

5.2 The size effect

The plot of size effect was obtained for notched and unnotched three point bend beams. The fracture energy adopted was GF = 150 [N/m]. Additional sizes of beams were considered, always with geometrically similar dimensions.

The nominal strength for each beam was obtained trough eq. (4) where P is the peak load, S = 2.5 d is the length of the beam, t is the thickness and h is the uncracked depth of the specimen.

$$\sigma_n = 1.5\frac{P\,S}{t\,h^2} \tag{4}$$

Eight sizes of beams were numerically tested for both notched and unnotched specimens and the results for nominal strength are shown in Table 4 and plotted in Figure 13.

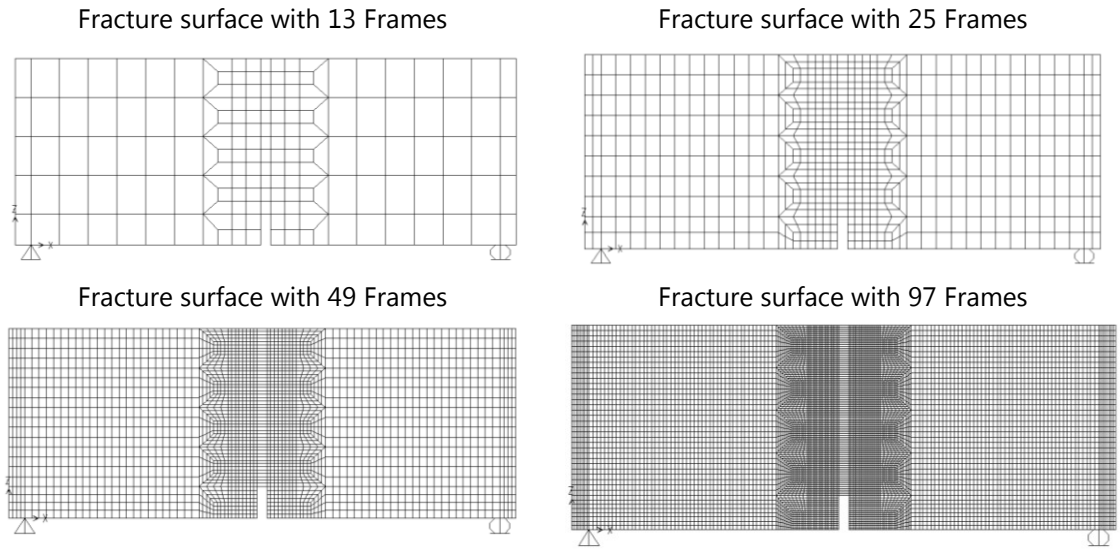

Figure 11: Four mesh refinement for beam of 38 [mm] of depth.

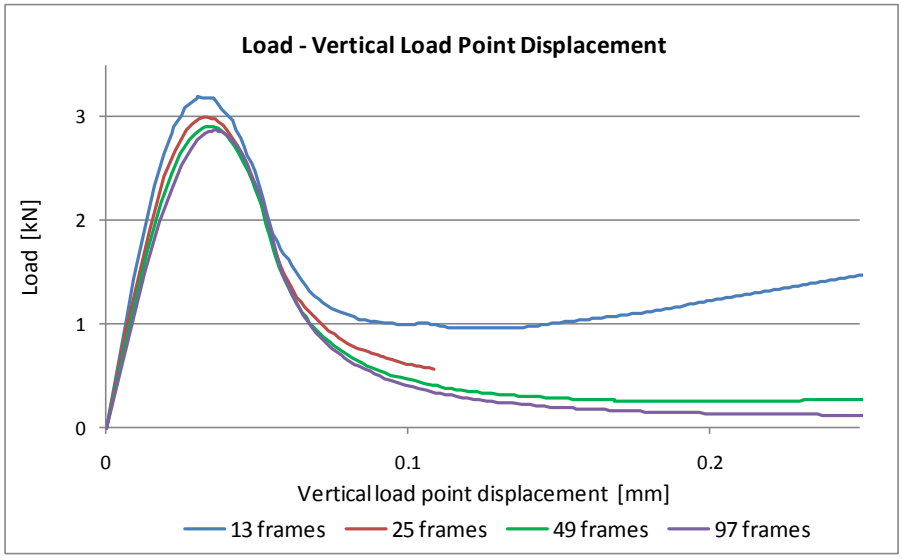

Figure 12: Load vs. vertical displacement for beam of 38 [mm] of depth with different levels of mesh refinement.

Number of frames in the predefined fracture surface	Peak load [kN]
13	3.19

25	3.00
49	2.90
97	2.86

Table 3: Peak load for different levels of discretization for a beam of 38 [mm] of depth.

Beam's depth [mm]	Nominal Strength of notched beams [kN/m^2]	Nominal Strength of unnotched beams [kN/m^2]
19	11967	11842
38	10695	10699
76	9368	9544
152	7937	8453
304	6619	7531
608	5306	6882
1216	4118	6489
2432	3114	6280

Table 4: Nominal Strength of notched and unnotched three point bend beams.

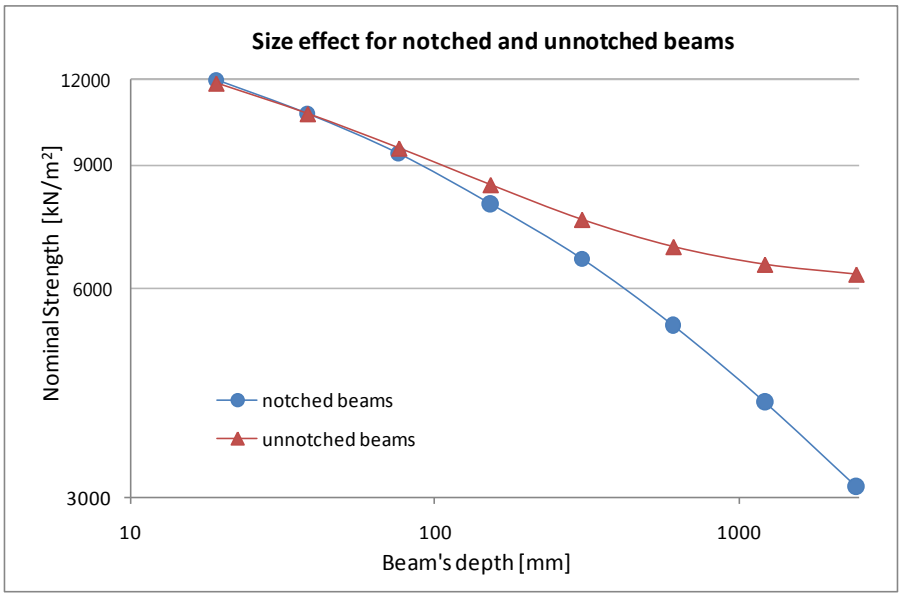

Figure 13: Size effect for notched and unnotched three point bend beams (logarithmic scale).

It can be observed that for small sizes the results tend to the nominal strength obtained by plastic limit analysis. For larger sizes the nominal strength of notched beams tend to results of linear elastic fracture mechanics and the nominal strength of unnotched beams tends to the modulus of rupture, as mentioned by Bažant and Planas (1998).

6 RESULTS FOR BILINEAR SOFTENING DIAGRAMS

Notched three point bend beams with 304 [mm] of depth were analyzed, all with fracture energy GF = 150 [N/m] and bilinear softening diagrams.

In the first sequence of numerical analysis the initial fracture energy was G_f = 60 [N/m] and the relation σ_k / f_t was adopted to be values of 0.05, 0.15, 0.25 and 0.33. The load-vertical displacement curves are shown in Figure 14.

For the second sequence the initial fracture energy was G_f = 100 [N/m] and the relations σ_k / f_t were assumed to be the same values as in the first sequence. The Figure 15 shows the load-vertical displacement curves for this analysis.

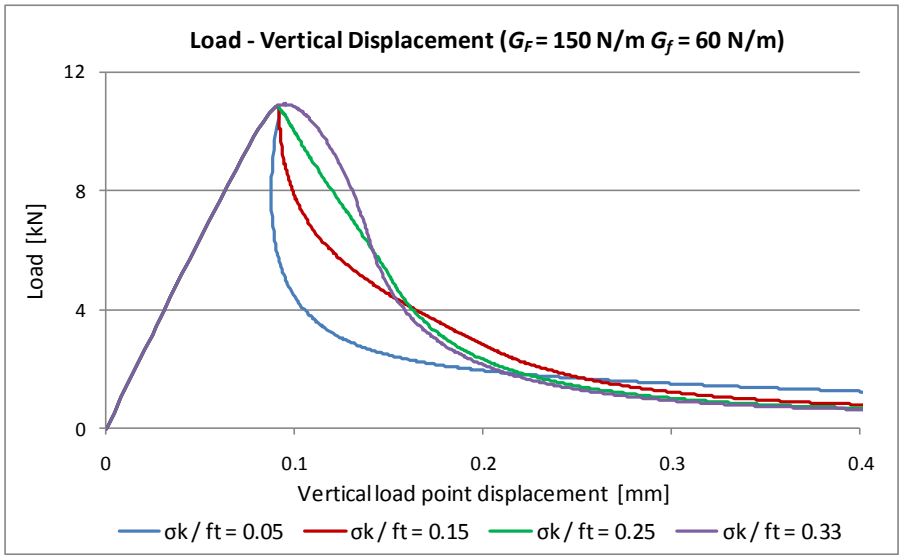

Figure 14: Load vs. vertical displacement for a beam with 304[mm] of depth, initial fracture energy G_f = 60 [N/m] varying the position of the kick point.

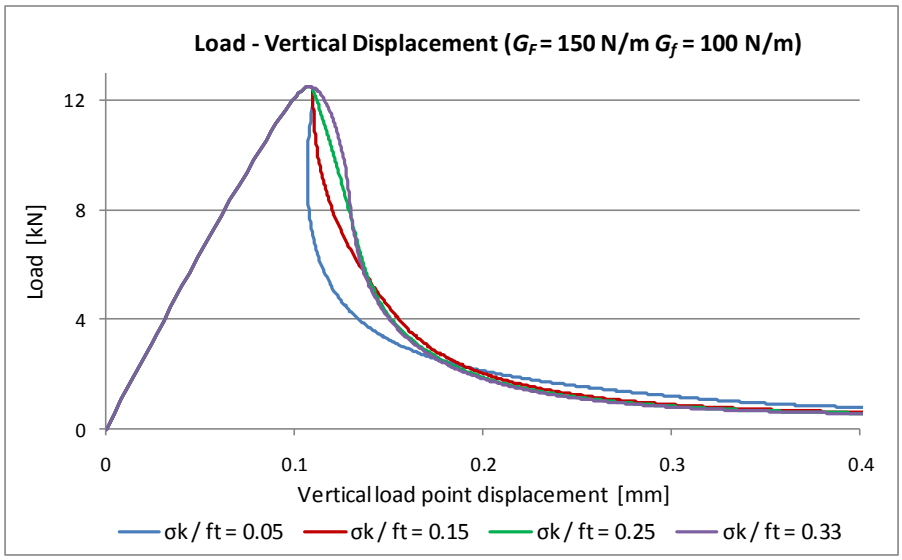

Figure 15: Load vs. vertical displacement for a beam with 304[mm] of depth, initial fracture energy G_f = 100 [N/m] varying the position of the kick point.

7 CONCLUSIONS

The cohesive crack method can be easily implemented in any program with elements having nonlinear constitutive relations, especially with softening stress-strain diagrams. This method is adequate for modeling fracture in quasi-brittle materials as the concrete.

Three point bent beams were analyzed in Sap2000, with shell elements used for the bulk linear material in the beams and frame elements with material nonlinear behavior for the pre-existing line in front of the fracture. The fracture energy is equal to the energy dissipated by the behavior nonlinear of the frames divided between their cross section. The results for load-displacement curves qualitatively agree with the experimental results observed in the literature when CMOD (crack mouth opening displacement) control is used (Caland, 2001). In specimens with smaller size the load-displacement curve presents a gradual decrease in load after the peak load is reached, with increasing displacements. For larger sizes the additional energy stored in the beam generates a snap-back behavior. In all specimen sizes the fracture energy computed from the resultant load-vertical displacement curve is in agreement with the input fracture energy.

As expected from the literature (Bazant and Planas, 1998), the peak load highly depends on the initial slope of the softening stress-strain diagrams mainly for small sizes. This can be observed even in the linear softening diagram since the peak load decreases as the fracture energy G_F decreases and therefore the slope of the softening diagram increases. The size effect is also well reproduced both for notched and unnotched beams with this method.

In order to adjust both the fracture energies and the peak loads measured in experimental tests, the bilinear softening diagram appears more suitable. However, it can be seen that the location of the kink point in this diagram affects the post-peak behavior, eliminating in some cases the snap-back of the resulting load-displacement curve. The influence of the relation σ_k / f_t is more pronounced when the relation G_F / G_f (fracture energy / initial fracture energy) is larger.

Even with the disadvantage that the fracture line has to be known a priori, this method constitutes a powerful tool that can get advantage of highly efficient commercial software to determine the peak load of special structures, since the parameters of the material needed to construct the softening stress-strain diagrams can be experimentally determined and compared with numerical analysis.

ACKNOWLEDGEMENT

The authors acknowledge to the Government agencies CNPq, CAPES and ANEEL for financial support.

REFERENCES

Bažant, Z.P., Concrete fracture models: testing and practice, *Engineering Fracture Mechanics*, 69:165-205, 2002.

Bažant, Z.P., Planas, J., *Fracture and size effect in concrete and other quasibrittle materials*, CRC Press LLC, 1998.

Caland, V.S., Resultados experimentais dos parâmetros de fraturamento para concretos de alto desempenho, *Thesis PUC Rio*, 2001.

CSI, Analysis reference manual for Sap2000, *Computers and Structures Inc.*, 2009.

Roesler, F., Paulino, G.H., Park, K, and Gaedicke, C., Concrete fracture prediction using bilinear softening, *Cement & Concrete Composites*, 29:300–312, 2007.